

# DESIGN OF BEAM PROFILE MONITOR USED AT THE Xi'an PROTON APPLICATION FACILITY (XiPAF)

D. Wang<sup>†</sup>, W. Chen, Z. M. Wang, M. W. Wang, Northwest Institute of Nuclear Technology, 710024, Xi'an, China

P. F. Ma, Y. G. Yang, Tsinghua University, 100084, Beijing, China

## Abstract

A pixel ionization chamber for beam profile monitor (BPrM) is designed and manufactured by a new technology. The detector will be installed on the beam line just upstream of the target device of XiPAF. It has many advantages such as high resolution, high radiation hardness and it can work as a real-time monitor to show the distribution of the delivered relative dose. The physics design and construction of the detector are described in this paper, and its performances are tested offline.

## INTRODUCTION

The Xi'an Proton Application Facility (XiPAF), located in Xi'an (China), is used for radiation hardness qualification of space electronics and devices. The slow extracted proton beam after a synchrotron is transported and tuned by a beamline named High Energy Beam Transport line (HEBT) [1]. Then the beam is extracted to experimental station in air after a metallic foil window, and the thickness of the window is about 100µm to preserve the high vacuum system of the beam transport system. Table 1 shows the main parameters of the proton beam in experimental station.

Table 1: Parameters of the Proton Beam

Parameter	Value	Unit
Energy	10~200	MeV
Flux	$10^5 \sim 10^8$	$\text{cm}^{-2} \text{s}^{-1}$
Beam size	$10 \times 10 \sim 100 \times 100$	$\text{mm}^2$

To fulfill the requirements of experiment of irradiating DUTs (devices under test), the extracted beam is semi-continuous and the beam intensity is from  $10^5$  to  $10^{10}$  particles per second. As shown in Table 1, the beam size is adjustable for different scales of DUTs. Such an irradiation method requires a stable, high resolution, and high radiation hardness BPrM, which can work as a real-time monitor to show the distribution of the delivered relative dose.

The first part of the paper describes the detector design and construction in detail, we have built a pixel ionization chamber, by a new technology, to be used as BPrM before DUTs. Secondly, some important performance parameters are tested or calculated. And finally in Section 4 we draw the conclusions of this work.

## DETECTOR DESIGN AND CONSTRUCTION

Reference. [2] shows an overview of the different detector systems used for slow extraction at the GSI synchrotron. Our detector has been designed to be placed upstream of the DUTs, The main constraints of the design of the detector are:

- as little as possible thickness to reduce the impact to proton beam;
- large sensitive area and dynamic range to suit for different beam sizes and intensities;
- good radiation hardness to achieve a long lifetime.

We find ionization chamber fits the beam parameters shown in Table 1, a gas-filled parallel plate ionization chamber can be constructed with extremely thin electrodes and windows. This paper uses a new technology, called Flexible Printed Circuit (FPC), to make the pixels segmented and to achieve signals brought out.

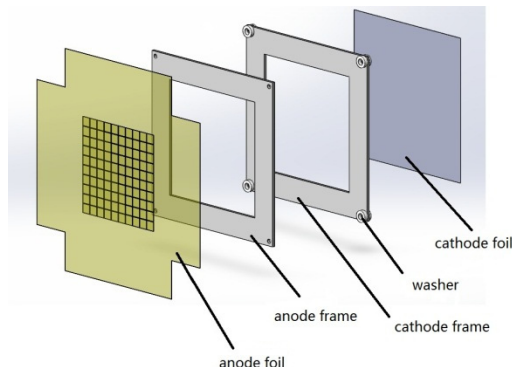


Figure 1: Exploded view of the chamber.

Figure 1 shows an exploded view of the chamber. The anode, the key component of this detector, is made of double-sided flexible circuit board. The anode consists of a 20 µm thick polyimide layer on which a 18 µm thick copper film has been deposited on both sides. The front side has been segmented into 256 square pixels, which consists of 64 small pixels, 128 middle pixels and 64 big pixels. The areas of these pixels are  $2.5 \times 2.5 \text{ mm}^2$ ,  $5 \times 5 \text{ mm}^2$  and  $10 \times 10 \text{ mm}^2$ , respectively.

Figure 2 shows the photograph of anode. Indeed we can design the number and shape of collection pixels, differently, as required. The tracks on back side are connected to pixels one-to-one through a conductive hole and bring the signals from the pixels to the connectors housed at the edge of the anode film. In Figure 2, we show the guard-ring

<sup>†</sup>Corresponding author: wangdi@nint.ac.cn

Content from this work may be used under the terms of the CC BY 3.0 licence (© 2018). Any distribution of this work must maintain attribution to the author(s), title of the work, publisher, and DOI.

This is a preprint — the final version is published with IOP

around the sensitive area, which can decrease leakage current by connecting to ground and keep electric field uniform between the electrodes.

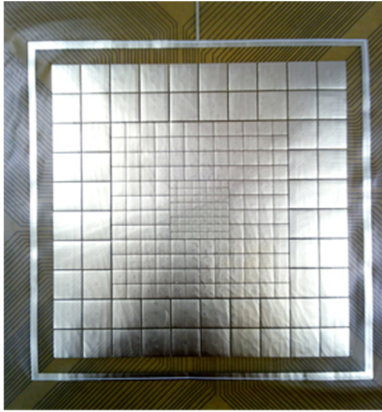


Figure 2: The anode foil consists of three kinds of pixels.

The cathode and windows are made of 6  $\mu\text{m}$  aluminized PET films, the thickness of the aluminum layer being below 1  $\mu\text{m}$ . They are glued on the copper printed frames by conducting resin. The electric field is generated by polarizing the cathode to a high voltage ( $HV$ ), which is about -300 V to -1000 V for different ionization intensities  $q$  and electrodes gaps  $d$ .

The relationship between collection efficiency  $f$  and  $HV$ ,  $q$ ,  $d$ , reported in Ref. [3], is given by

$$f = \frac{1}{1 + \frac{1}{6} \xi^2}, \quad (1)$$

putting

$$\xi = \sqrt{\frac{\alpha}{ek_1k_2}} \cdot \frac{d^2 \sqrt{q}}{HV} = m \frac{d^2 \sqrt{q}}{HV}, \quad (2)$$

where  $k_1$  and  $k_2$  are the mobilities of positive and negative ions, respectively, and  $\alpha$  is their recombination coefficient,  $m$  is a constant characteristic of the gas at the given temperature and pressure.

Usually for a transmission ionization chamber, the signal response is proportional to the electrodes gap  $d$ . However we cannot increase  $d$  unboundedly to obtain a stronger signal because of the transverse diffusion for a pixel ionization chamber. The diffusion can be simulated by the Garfield program, which was developed firstly for simulation of 2-D drift chamber at CERN [4]. The result shows that in nitrogen the electron's diffusion is 0.4mm per 1 cm drift distance when the electric field strength is 1 kV/cm. And 1.3 mm, 0.6 mm for argon and P10 gas (90% argon and 10% methane), respectively. So nitrogen is recommended as the working gas, whose diffusion is acceptable in comparison with the pixel size 2.5 mm.

Therefore, we select  $d=1$  cm and  $HV=1000$  V to achieve an ideal collection efficiency, which is close to 100%, as shown in Figure 3. This figure gives the collection efficiency in a plane-parallel ionization chamber exposed to continuous radiation as a function of high voltage. The four pictures in Figure 3 corresponding to four regular

electrodes gaps and the different colors mean different beam fluxes of XiPAF.

Figure 4 shows an inner view of the assembled chamber, the external dimensions of the detector are (28 $\times$ 28 $\times$ 4) cm, which is easily inserted in the experiment station.

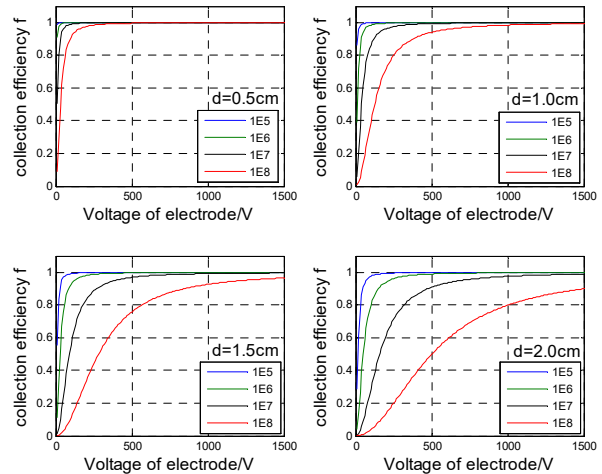


Figure 3: Collection efficiency as a function of HV.

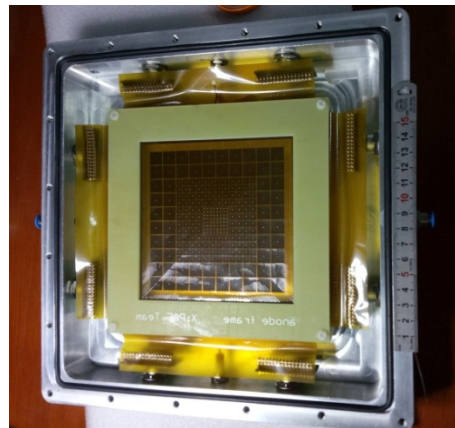


Figure 4: Inner view of the assembled chamber.

## DETECTOR CHARACTERIZATION

### Leak Current Test

The number of electrons created in the gas volume is of the order of  $10^3$ /proton, and the drift time of positive ions is about 1 ms, which is much longer than the interval period of the slow extracted beam. So it can be regarded as a DC-beam for this detector, which results in a weak output current in the range of pA~ $\mu\text{A}$ . And the minimum of the range is limited by leak current, so it's important to test the leak current of each pixel channel.

We connected cathode to  $HV$  about -1.5 kV and measured the leak current channel by channel by IC101, a digital electrometer produced by Pyramid Technical Consultants [5]. Figure 5 shows the leak current data of 64 channels, which consist a quarter of the sensitive area. The values are all below 1 pA, which is an acceptable level of leak current.

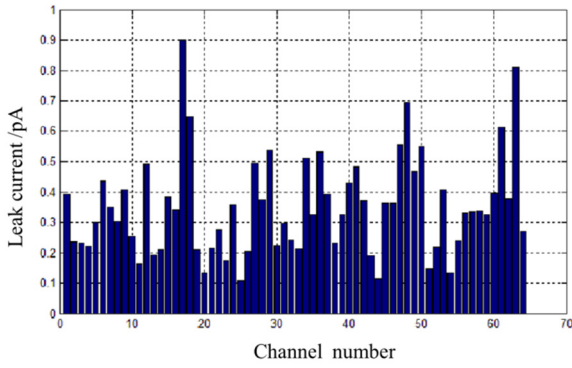


Figure 5: Leakage current of 64 channels.

### Assessment of Thickness

Equivalent water thickness (WET) value is an important part of transmission detector, which is given by

$$WET = \sum_{i=1}^n \frac{R_{water}}{R_i} \times d_i, \quad (3)$$

where  $d_i$  is thickness of material  $i$ , and  $R_i$  is the depth of the proton Bragg peak in material  $i$ , which is simulated by the Monte-Carlo transport code TRIM [6]. The results are shown in Table 2, the WET value is about 300  $\mu\text{m}$  for 10 MeV and 200 MeV protons, which has reached international advanced level.

Table 2: The WET Value of All Materials

Mat.	$d_i$ [ $\mu\text{m}$ ]	$R_i$ [cm] @200 MeV	$R_i$ [ $\mu\text{m}$ ] @10 MeV	$WET_i$ [ $\mu\text{m}$ ] @200 MeV	$WET_i$ [ $\mu\text{m}$ ] @10 MeV
Cu	36	4.35	243	211.03	177.78
Al	6	12.15	624	12.59	11.54
PET	18	19.75	936	23.24	23.08
Kapton	30	19.75	936	38.73	38.46
N <sub>2</sub>	35910	23250	1116000	39.38	38.61
Total	36000	/	/	324.99	289.47

### Thermal Aspects

Energy loss in the detector materials will result in thermal effects, for DC-beams, materials will finally reach to the steady state, where the radiated thermal power is equal to the deposited power. If we just consider thermal radiation, a conservative estimation of material temperature  $T$  can be done by the following equation,

$$F \cdot \frac{dE}{dx} \cdot \Delta x \left[ \frac{W}{\text{cm}^2} \right] = \varepsilon \sigma (T^4 - T_e^4) \quad (4)$$

where  $F$  is the beam flux;  $\Delta x$  is the thickness of material;  $dE/dx$  is the stopping power of material;  $\varepsilon$  is the emissivity;  $\sigma = 5.67 \times 10^{-8} [\text{W}/\text{m}^2\text{K}^4]$  is the Stefan-Boltzmann constant,  $T_e$  is the temperature of the environment. The result shows temperature rises of electrodes and windows are less than 1 K, so the thermal effects are negligible.

## SUMMARY

In this paper we report the design and construction of a pixel ionization chamber used as BPrM. The 256 pixels cover a total area of  $(100 \times 100) \text{ mm}^2$ . The geometric intrinsic resolution of the prototype is 2.5 mm. The WET value is about 0.3 mm and the other important characterizations are tested. This detector is a promising application in the area of on-line beam profile monitor.

## REFERENCES

- [1] G. R. Li *et al.*, "Design of the key parameters in an advanced radiation proton synchrotron", *Modern Applied Physics*, vol. 6, no. 2, pp. 85-89, 2015.
- [2] P. Forck, Lecture Notes on Beam Instrumentation and Diagnostics, Joint University Accelerator School (JUAS), Geneva, Switzerland, 2011.
- [3] F. H. Attix, "Introduction to radiological physics and radiation dosimetry", Weinheim, Germany, Wiley, 1986.
- [4] R. Veenhof, "Garfield, recent developments", *Nuclear Instruments & Methods in Physics Research Section A*, vol. 419, pp. 726-730, 1998.
- [5] <http://www.ptcusa.com/products/17>
- [6] <http://www.srim.org/>.

Content from this work may be used under the terms of the CC BY 3.0 licence (© 2018). Any distribution of this work must maintain attribution to the author(s), title of the work, publisher, and DOI.

This is a preprint — the final version is published with IOP